Pramāṇa, Vol. 22, Nos 3 & 4, March & April 1984, pp. 313–328. © Printed in India.

Thermal neutron polarisation

N S SATYA MURTHY and L MADHAV RAO
Nuclear Physics Division, Bhabha Atomic Research Centre, Bombay 400 085, India

Abstract. The basic principle for the production of polarised thermal neutrons is discussed and the choice of various crystal monochromators surveyed. Brief mention of broad-spectrum polarisers is made. The application of polarised neutrons to the study of magnetisation density distributions in magnetic crystals, the dynamic concept of polarisation, principle and use of polarisation analysis, the neutron spin-echo technique are discussed.

Keywords. Thermal neutrons; polarisation; polarised beam; multilayer structures; neutron polarisation; radio frequency spin flipper; Mezei spin flipper; beam diffractometer; spin-echo spectrometry.

1. Introduction

Some of the earliest experimental studies of the polarisation of neutrons for the purpose of verifying the theory of scattering of thermal neutrons passing through crystalline materials were conducted in the late 1930s and early 1940s. In these types of experiments, velocity selection was accomplished using the rotating shutter and the pulsed cyclotron time of flight methods. The late 1940s saw the advent of research reactors and the use of reactor neutrons and crystal spectrometry techniques to study condensed matter in general and magnetism in particular. Production of polarised neutrons using this technique was first reported by Shull (1951). Since then the last three decades have seen a fascinating development of various techniques to produce polarised neutrons and apply them with considerable success to a variety of problems in magnetism.

Here, we survey the methods to produce and control the polarisation of neutrons and describe briefly its application to a variety of physical problems with due reference to Indian contributions.

2. Description of a polarised beam of neutrons

The polarisation of a neutron beam is defined to be twice the average value of the neutron spin in the beam. That is,

$$\mathbf{P} = 2\langle \hat{\mathbf{S}} \rangle = \langle \hat{\boldsymbol{\sigma}} \rangle, \tag{1}$$

where

$$\hat{\sigma}_x = \begin{pmatrix} 0 & 1 \\ 1 & 0 \end{pmatrix}; \quad \hat{\sigma}_y = \begin{pmatrix} 0 & -i \\ i & 0 \end{pmatrix}; \quad \hat{\sigma}_z = \begin{pmatrix} 1 & 0 \\ 0 & -1 \end{pmatrix}. \tag{2}$$

For an unpolarised beam $\mathbf{P} = 0$, for a completely polarised beam $|\mathbf{P}| = 1$. In a partially polarised beam, $0 < |\mathbf{P}| < 1$. We cannot assign a wavefunction to the spin state of a

neutron in a partially polarised beam. A partially polarised beam of neutrons can only be defined by some probability distribution. The physical attributes of such a system, called the 'mixed' system, can be conveniently described in terms of a density matrix operator $\hat{\rho}$. We first construct the density matrix for a single neutron and then obtain the density matrix operator for the beam of neutrons by averaging over the density matrices of the individual neutrons.

The most general form of the spin wavefunction for a neutron can be expressed as

$$\chi = a\chi_{\uparrow} + b\chi_{\downarrow}, \tag{3}$$

where $\chi_{\uparrow}$ and $\chi_{\downarrow}$ are eigenfunctions of $\hat{\sigma}_z$. Obviously

$$|a|^2 + |b|^2 = 1. \tag{4}$$

Physically, $|a|^2$ and $|b|^2$ represent the probabilities that a measurement of the z component of a spin will show that the spin is parallel ($\uparrow$) or antiparallel ($\downarrow$) to the z direction. There will always exist a direction defined by the unit vector $\hat{\xi}$ such that

$$(\hat{\boldsymbol{\sigma}} \cdot \hat{\boldsymbol{\xi}})\chi = \chi,$$

i.e. the spin is fully aligned along $\hat{\xi}$.

We define the density matrix operator $\hat{\rho}$ as

$$\hat{\rho} = \chi\chi^{+} = \begin{pmatrix} |a|^2 & ab^* \\ ba^* & |b|^2 \end{pmatrix} \tag{5}$$

$\hat{\rho}$ is Hermitian and has a unit trace, $\mathrm{Tr}\,\hat{\rho} = 1$. $\hat{\rho}$ being a 2×2 Hermitian matrix, it can be expanded in terms of the unit matrix I and the Pauli matrices σ^a with real expansion coefficients

$$\hat{\rho} = \tfrac{1}{2}(I + \mathbf{P} \cdot \hat{\boldsymbol{\sigma}}), \tag{6}$$

in which we define

$$\begin{aligned} P_x &= 2\,\mathrm{Re}\,(a^*b), \\ P_y &= 2\,\mathrm{Im}\,(a^*b), \\ P_z &= |a|^2 - |b|^2. \end{aligned} \tag{7}$$

In a beam of neutrons now, each individual neutron will have its own spin state described by the density matrix. The polarisation of the beam will be the average over the polarisation of each neutron. Thus if the jth neutron has a polarisation P_j and there are n neutrons, the polarisation P of the beam is

$$P = \frac{1}{n}\sum_j P_j. \tag{8}$$

The magnitude of $\mathbf{P}$ must lie between zero and unity and the density matrix of the beam is clearly $\hat{\rho} = \frac{1}{2}(I + \mathbf{P} \cdot \hat{\boldsymbol{\sigma}})$, $(0 \leqslant |\mathbf{P}| \leqslant 1)$. Now $\langle \hat{\rho} \rangle = \mathrm{Tr}\,\hat{\rho}\hat{\rho} = \frac{1}{2}(1 + |\mathbf{P}|^2)$ from which it follows that

$$\langle \hat{\rho} \rangle \geqslant \tfrac{1}{2}, \tag{9}$$

and since $|\mathbf{P}|^2 \leqslant 1, \quad \langle \hat{\rho} \rangle \leqslant 1.$ (10)

The equality in (9) is satisfied for an unpolarised beam ($\mathbf{P} = 0$) while the equality in (10) is satisfied for a fully polarised neutron beam.

3. Production of polarised beam of thermal neutrons

In an operational sense, we can define thermal neutrons as those neutrons whose wavelength range is such that they can be conveniently Bragg-scattered from single crystals. This wavelength range lies roughly from 0·5 Å to 6 Å. In magnetically ordered crystals, because of the magnetic periodicity of the lattice, we can expect thermal neutrons to be Bragg-scattered, in addition to the normal Bragg scattering that will occur due to the nuclear or "chemical" periodicity of the lattice.

The theory of scattering of neutrons by magnetic crystals was first developed by Halpern and Johnson (1939). They, however, considered only uniaxial ferromagnetic and antiferromagnetic materials. Later, Maleev (1961), Blume (1963) and Steinsvoll (1963) treated the problem in a more general way using Green function techniques and the spin density matrix description. These treatments take into account terms which were neglected by Halpern and so bring out the intensity and polarisation features of neutron scattering by more complicated magnetic structures. However, for the purpose of the present discussion, the theory of Halpern and Johnson is quite adequate. According to them, the intensity of the scattered neutrons by an ordered magnetic crystal is given by

$$I \sim N^2 + 2NM\,\mathbf{q}\cdot\boldsymbol{\lambda} + M^2q^2, \tag{11}$$

where N and M are the nuclear and magnetic structure factors, $\mathbf{q}$ is the magnetic interaction vector and $\boldsymbol{\lambda}$ is the unit vector along the neutron polarisation direction. The term $\mathbf{q}$ is defined by the relation

$$\mathbf{q} = \hat{\mathbf{e}}(\hat{\mathbf{e}}\cdot\hat{\boldsymbol{\eta}}) - \hat{\boldsymbol{\eta}}, \tag{12}$$

where $\hat{\mathbf{e}}$ and $\hat{\boldsymbol{\eta}}$ on the unit vectors along the directions of the scattering vector and magnetic moment orientation respectively. When the crystal is magnetised to saturation at right angles to the scattering vector,

$$\hat{\mathbf{e}}\cdot\hat{\boldsymbol{\eta}} = 0,$$

and hence $$\mathbf{q} = -\hat{\boldsymbol{\eta}} \text{ and } |\mathbf{q}|^2 = 1. \tag{13}$$

Also,

$$\mathbf{q}\cdot\hat{\boldsymbol{\lambda}} = -\hat{\boldsymbol{\eta}}\cdot\hat{\boldsymbol{\lambda}} = \pm 1$$

depending on whether the neutron polarisation is directed opposite the magnetic moment orientation or is parallel to it. The scattered intensities for the two neutron spin states (analysed such that $\mathbf{q}\cdot\hat{\boldsymbol{\lambda}} = \pm 1$) that make up an unpolarised incident neutron beam can be written as

$$\begin{aligned} I_+ &= 4\pi(N+M)^2 \text{ with } \mathbf{q}\cdot\hat{\boldsymbol{\lambda}} = +1, \\ \text{and} \qquad & \qquad (14) \\ I_- &= 4\pi(N-M)^2 \text{ with } \mathbf{q}\cdot\hat{\boldsymbol{\lambda}} = -1. \end{aligned}$$

With unpolarised incident radiation, the total scattered intensity $I = (I_+ + I_-)$ becomes half of the sum of the two spin-state cross-sections or

$$I \sim 4\pi(N^2 + M^2). \tag{15}$$

Thus the intensity of the Bragg-scattered beam will be the sum of the intensities of nuclear Bragg and magnetic Bragg scattering. However, if there happens to be a Bragg plane in the crystal for which the magnitudes of the nuclear structure factor N and

magnetic structure factor M almost match (*i.e.* $|M| \simeq |N|$) then clearly such a crystal will preferentially scatter neutrons of only one spin state and thus will yield a highly polarised neutron beams whose polarisation P can be expressed as

$$P = \frac{I_+ - I_-}{I_+ + I_-} = \frac{2NM}{N^2 + M^2}. \tag{16}$$

When $|N| = |M|$, $P = 1$, and the scattered neutron beam is fully polarised. Thus this technique offers us a method of achieving simultaneous monochromatization and polarisation of a thermal neutron beam. Although such a fortuitous equivalence of the nuclear and magnetic structure factors occurs in a few crystals naturally (Fe_3O_4, Co(Fe)), to-day a number of neutron polarisers have become available because of isotopic alloying or using a solid solution range to achieve ideal cancellation of N and M and thereby, perfect polarisation.

The detection and utilisation of such a polarised neutron beam was first discussed by Shull (1951) and Stanford *et al* (1954) and the first polarised neutron spectrometer based on this principle was built by Shull and his colleagues (1959) at the M.I.T. Reactor in USA.

Historically, the first magnetic crystal to be tested for its polarisation efficiency was Fe_3O_4, using its (220) planes (Shull 1951). The best polarisation efficiency obtained was only 95%. The next crystal that was tested was fcc cobalt ($Co_{0.92}Fe_{0.08}$) whose (200) plane theoretically should yield a polarisation efficiency of 99·2%. The high absorption cross-section of cobalt limits the effective thickness of the monochromator crystal to about 2 to 3 mm and this crystal is invariably used in symmetric transmission geometry. Experimentally it has been observed that the polarising efficiency of a given magnetic crystal is quite sensitive to the surface finish of the crystal. Co(Fe) being metallic, it is rather easy to polish its surface to a mirror finish and polarisation efficiency of better than 99% has been achieved.

A decided advantage to the use of Co(Fe) polarising crystals lies in their greater neutron reflectivity compared to the (220) Fe_3O_4 reflection. This arises because of the more favourable crystal structure factor and the greater density of magnetic scattering atoms. Moreover, the higher order contaminant neutrons are largely absent in Co(Fe). The magnetic structure of Fe_3O_4 is such that the (440) reflectivity is approximately 15 times larger than the (220) reflectivity and hence in scattering neutrons of wavelength λ from the (220) reflection there is a strong $\lambda/2$ component. The absolute sense of the neutron polarisation from Co(Fe) and Fe_3O_4 are opposite (with reference to the same magnetising field direction). The $\lambda/2$ component is partially polarised in the opposite direction and it is necessary to absorb this with a suitable filter such as Pu filter for $\lambda \simeq 1{\cdot}05$ Å, and this necessarily absorbs some of the desired intensity as well. This problem does not arise in the case of the (200) Co(Fe) reflection since the (400) crystal structure factor is of the same order as that of (200) and no enhancement of the $\lambda/2$ component is thus obtained. Thus the second order contamination in a polarising reflection is doubly undesirable. It also affects the flipping efficiency—when reversing the neutron polarisation, as this is also wavelength-dependent.

The Heusler alloys, Cu_2MnAl and Fe_3Si are two materials that have similar characteristics as polarisers and which can give higher reflectivities than Co(Fe). Both form superlattices based on fcc structures and in each case the (111) reflection is matched. Matching of the nuclear and magnetic scattering depends critically on the state of order, since the nuclear amplitude is the difference between the scattering at two

different atomic sites. In both materials the nuclear structure factor of the (222) reflection is significantly higher than that of (111), so that half wavelength contamination can be a problem (Delapalme *et al* 1971). Intensity enhancement factor of atleast 2·5 with a polarising efficiency of 96 % has been achieved in Cu_2MnAl *vis-a-vis* Co(Fe). Because of its large d spacing, Cu_2MnAl is conveniently used to obtain polarised beams in the wavelength region $\lambda \sim 4$ Å using cold neutron guide tubes where the problem of $\lambda/2$ contamination does not arise since the neutron beams provided by these guide tubes have a wavelength cut off around 3 Å.

Iron is an alternative to Co(Fe) since it has a similar low d spacing and high focussing angle but lower absorption, but natural iron has too large a nuclear scattering amplitude ($0{\cdot}951 \times 10^{-12}$ cm). However a single crystal of Fe enriched in Fe^{57} ($b = 0{\cdot}23 \times 10^{-12}$ cm) and 3 % Si was fabricated at the Oak Ridge National Laboratory, USA and tested out to provide excellent polarisation in the (110) reflection with an intensity gain of 4 over that of Co(Fe). Clearly, such a polarising monochromator is beyond the reach of most laboratories and cheaper alternatives have been pursued. Recently, Bednarski *et al* (1980) have tested the polarising efficiency of the (111) reflection from a large single crystal of $Fe_{3-x}Mn_xSi$ ($x = 0{\cdot}05$) and have found it to be 95 %. The intensity is a factor between 2 and 3 higher than that obtained from a single crystal of Co(Fe). They obtained a similar value from the (222) reflection of an ordered Li-ferrite single crystal ($Li_{0{\cdot}5}Fe_{2{\cdot}5}O_4$).

A cheaper alternative for a high focussing angle polariser may well result from current research into rare earth transition metal alloys. Rare earth magnetic moments can be large, up to $\sim 10\,\mu_B$ and their scattering factor curves fall more slowly with increasing $\sin\theta/\lambda$ than do those of the 3d electrons because of their compact electronic distribution. It should therefore be possible to find a material with a matched reflection having a low d spacing yet still giving good reflectivity. Rare earth alloys commonly exhibit high magnetic anisotropy, which would limit the choice of magnetisation direction and might require a high field for saturation. Again, some rare earth elements are unsuitable because of their large absorption factors for neutrons. Schweizer *et al* (1979) have concentrated their efforts on the cubic Laves-phase $HoFe_2$ where the (620) and (444) reflections promise to give good results. The easy direction of magnetisation in $HoFe_2$ is $\langle 001 \rangle$ so that (620) reflection is to be preferred for this reason; unfortunately its reflectivity is around 50 % of that for (444). The latter reflection can however be used if some Ho is replaced by Tb which produces an easy direction of magnetisation along $\langle 110 \rangle$ and only reduces the expected beam polarisation to 0·97. Actual performance tests regarding neutron beam polarisation and intensity using large single crystals of these Laves phase $HoFe_2$ and $Ho(Tb)Fe_2$ materials have not yet been carried out.

3.1 *Broad spectrum polarisers*

At wavelengths beyond the Bragg cut-off of conventional polarisers, recourse can be made to spin-dependent neutron optics in the form of polarising mirrors or guides. In a magnetic medium, the neutron refractive index depends upon the neutron spin state relative to the magnetic induction. By a suitable choice of material, the refractive index can be made to be slightly less than unity for only one spin state; a totally reflecting mirror of this material will then act as a polariser. (Hayter *et al* 1976). The more fundamental problem of mirror reflection is that the critical angle is very small and

depends linearly on the wavelength. Typically θ_c is about 30′ at 6 Å; and the divergence limitation is severe at shorter wavelengths. This problem can be resolved by the 'supermirror' idea of Mezei (1976). An evaporated multilayer film system is used which is analogous to the multilayer interference coatings used in light optics. An enhancement of the critical angle by a factor of atleast 3 is possible, so that mirror polarisers would become useful at short wavelength; at long wavelengths they would also provide wide divergence analysers. The problem of producing intense white polarised beams with reasonable divergence thus appears to be solved.*

3.1*a Polarising multilayer structures* Evaporated films may also be used to build up multilayer two-dimensional synthetic crystals which act as long wavelength monochromators (Schoenborn *et al* 1974). If alternate layers are of magnetic material whose refractive index for $1-\rangle$ neutrons is matched to that for the interlaced (nonmagnetic) layers, only $1+\rangle$ neutrons will see a periodic structure and hence Bragg reflections will be polarised. These polarisers have the advantage of monochromating in a controllable way, since the lattice spacings can be chosen to suit any particular problem.

Very recently, in the course of investigating magnetic structure and magnetic form factors in Mn_4N powder, using polarised neutrons, Sumaamidjaya *et al* (1983) observed that the first two of its reflections, the (100) and (110) present themselves as two good candidates for providing polarised neutrons. By evaluating the magnetic structure factors for these two reflections they predict a polarisation efficiency of 99·6 % and 94·8 % for the (100) and (110) planes respectively. It is interesting to observe that the polarisation state for these 2 planes is in opposite directions. This then offers the fascinating possibility of producing polarised monochromatic neutrons of either state of polarisation by switching from one reflection to the other, without the use of electronic flipping devices. (It has to be recognised however, that the two reflections will provide different wavelengths for the same monochromator setting angle). The *d* spacings of these two polarising reflections lie close in value to that of the (111) plane in Cu_2MnAl. Mn_4N may therefore be a good alternative to Cu_2MnAl in the production of polarised beam in the wavelength region around 4 Å. However, good single crystals of Mn_4N have not been grown so far.

Table 1 summarises briefly the features of the principal polarising monochromators discussed above.

4. Control of neutron polarisation

Neutron polarisation can be maintained by providing a continuous magnetic guide field (~ 100 Oe) along the path of the neutron beam. Initially, both these magnetic fields and the direction of neutron polarisation will be common to the field direction in the polariser. Subsequently, the direction of polarisation can be changed by providing a slow rotation of the magnetic guide field, such that the rate of change of the field vector **H** acting on the neutron in this adiabatic guide region is slow compared to the Larmor

*Polarising filters were earlier used as broad spectrum polariser. Such filters based on the polarised nuclei: the proton in $La_2Mg_3(NO_3)_{12}\cdot 24\,H_2O$, LMN or the ^{149}Sm nuclei (Luschikov *et al* 1970, Williams 1974) are expensive to construct and operate mainly due to the low temperatures involved (< 1K for LMN, < 0·02 K for ^{149}Sm). These are therefore being increasingly replaced by other devices discussed in this section.

Table 1. Properties of a number of different polarising monochromators.

	Co(Fe)	Cu_2MnAl	Fe_3Si	$Fe_3Si(Mn)$	$Li_{0.5}Fe_{2.5}O_4$	$Fe^{57}(Fe, Si)$	Mn_4N
Matched reflection	200	111	111	111	222	110	100 110
d spacing (Å)	1·76	3·43	3·27	3·24	2·40	2·03	3·87 2·73
$2\theta_B$ for 1 Å neutrons	33·1°	16·7°	17·6°	17·7°	24°	28·6°	14·9° 21°
Linear absorption coefficient (cm^{-1}) for 1 Å neutrons	2·2	0·26	0·12	0·13	0·07	0·20	0·55
Crystallographic quantity Q (cm^{-1})	0·0064	0·0029	0·0017	0·0017	0·0068	0·0071	0·0038 0·0021
Optimal thickness of monochromator (mm)	1·9	2·5	5·5	5·5	12	5·3	1 1·5
Integrated reflectivity	0·0008	0·0032	0·0009	0·0012	0·027	0·010	0·0019 0·0011
Polarisation achieved (achievable); Polarising field ↑	0·99↑	0·97↓	0·96↑	0·95↓	0·95↑	0·95↑	(0·996)↓ (0·948)↑
Intensity gain experimentally got	1	2·5	2	2·5	2·5	4	(2·4) (1·4)
Figure of merit = Intensity gain × polarisation	1	2·45	1·94	2·40	2·40	3·84	(2·41) (1·34)

frequency w_L of the neutron

$$\frac{d\theta_H}{dz}\frac{dz}{dt} \ll w_L = \gamma_n |\mathbf{H}| \tag{17}$$

where θ_H is the angle between the magnetic field **H** and the neutron beam direction z; γ_n is the neutron gyromagnetic ratio ($-1{\cdot}83 \times 10^4$ rad. $\sec^{-1}$ Oe^{-1}).

Spin flippers operate on one of two principles: (a) systems in which the neutron spin undergoes a number of Larmor precessions while traversing a well-defined distance in a fixed magnetic field (b) systems in which the neutron spin experiences a fast magnetic field reversal, which it cannot follow adiabatically, so that the neutron polarisation is reversed with reference to the direction of the guide field.

4.1 *Radio frequency spin flipper*

The radio frequency spin flipper used by Nathans *et al* (1959) is an adaptation of the Alvarez-Bloch resonance technique and was first described by Stanford *et al* (1954); it has since been extensively used in polarised neutron diffractometry. The radio frequency field H_1 is applied perpendicular to the neutron polarisation direction and is matched to w_L in a region of highly uniform magnetic field, H_0. The rf current is adjusted in amplitude to achieve complete spin reversal in a well-defined coil length or neutron transit time. In practice, H_0 is usually some 0·01 to 0·02 T and $H_1 \sim 0{\cdot}02\, H_0$. The wavelength dependence of the rf flipper is such that its use should be restricted to cases when $\Delta\lambda/\lambda \leqslant 0{\cdot}1$. In particular, any $\lambda/2$ component in an otherwise monochromatic beam is effectively depolarised on passing through the flipper, since its polarisation is rotated by $\pi/4$ (Jones and Williams 1977). A flipping efficiency of nearly 100% can be easily achieved with the rf flipper, given some care in its design and construction.

4.2 *Mezei spin flipper*

The direct current spin flipper first suggested by Mezei (1972) is illustrated in figure 1. It

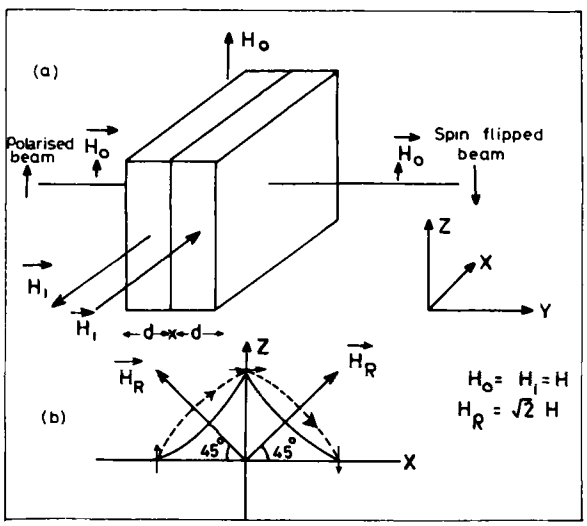

Figure 1. (**a**) Mezei flipper coils (**b**) the rotation of the neutron spins in the two coils.

consists of two rectangular coils of thickness d mm, one placed immediately behind the other with their axes perpendicular to both the neutron beam direction and a magnetic guide field H_0. The coils produce magnetic field H_1 along their axes which are equal and opposite in direction and, in the usual arrangement, these fields are also equal to the guide field H_0, *i.e.* $H_1 = H_0 = H$. If the coil width is such that

$$d = \pi v/\gamma_n H\sqrt{2}, \tag{18}$$

where v is the neutron velocity in mm sec^{-1}, then all these neutrons suffer precisely half a Larmor precession around a $\pi/2$ cone in each coil and hence undergo complete spin reversal on traversing both the coils (see figure 1). Badurek *et al* (1973) have investigated the sensitivity of this kind of flipper to magnetic field variations, and Van Laar *et al* (1976) showed that (18) is in error since it neglects the presence of the return fields outside the two coils. Nevertheless, a flipping efficiency of 0·997 has been achieved by Badurek *et al* using this flipper.

Examining the neutron scattering equations from non-collinear magnetic structures of Blume and others, Nityananda and Ramaseshan (1971) theoretically predicted a feature which should be observed in single domain helimagnetic crystals (such as Holmium at low temperatures) in the transmitted neutron beam for all wavelengths when the crystal orientation does not satisfy the Bragg condition. They showed that the phase of the transmitted neutron wave is different for the two cases when the polarisation is parallel ($+z$) and antiparallel ($-z$) to the axis of the belix. Consequently, if the incident polarisation is in the x-y plane, then on emerging from the crystal the neutron polarisation is rotated in this plane, the angle of rotation being proportional to the thickness of the crystal traversed. The magnitude of the rotation is a function of the pitch of the helix and the atomic magnetic moment. In Dy or Ho for example, they predicted, using a simplified model, a polarisation rotation of the order of 300 degrees per mm. In this sense, this 'device' can be called a spin turner much like a Nicol prism, rather than a spin flipper. However, a practical realisation of this concept of spin-turning is beset with many problems. Furthermore, severe depolarisation of the beam is likely to occur as it enters and leaves the surface of the crystal.

4.3 *Non-adiabatic spin flipper*

Methods hitherto discussed to flip or rotate the neutron polarisation are based on the adiabatic principle. We shall briefly discuss a non-adiabatic spin flipper devised and installed by Tasset. Non-adiabatic spin flippers reverse the magnetic guide field as seen by the neutron in a time that is much shorter than its Larmor period. A spin-flip transition ($\mathrm{d}\theta_H/\mathrm{d}z = \pi$) is most easily achieved for fast neutrons, velocity v, in low magnetic fields where

$$\pi v \gg \gamma_n H d$$

d, being the distance over which the magnetic discontinuity occurs.

In the flipping process the neutron spin vector can be considered as spatially fixed as it traverses the magnetic discontinuity and it is therefore reversed with respect to its guide field after passing through the discontinuity. In addition to their usefulness with polychromatic beams, non-adiabatic spin flippers have the advantage that they have no special magnetic field homogeneity or stability requirements and they can be easily made efficient over large beam areas ($\sim 10\,\mathrm{cm}^2$). Figure 2 shows the schematic

arrangement of permanent magnet guides A and E which provide the initial and final vertical direction of polarisation. A superconducting sheet of niobium (C) is used to isolate the fields from two adjacent sections of the guide field (B and D). Electromagnetic windings provide the two short guide field regions B and D on either side of the superconducting sheet C, which is cooled by conduction from a liquid He reservoir in a large capacity cryostat. Switching the current direction in the first of these two coils introduces an adiabatic rotation of π in the neutron spin direction in the gap between the regions A and B and this reversed polarisation is transmitted by the foil.

5. Polarised beam diffractometer

Nathans *et al* (1951) were the first to describe the principles of the polarised beam neutron diffractometer. Figure 3 is a schematic diagram of a typical diffractometer. Since data are normally required to values of $\sin\theta/\lambda$ in excess of 0·8 Å^{-1}, the incident beam has a wavelength of 1 Å or less. Extinction is the largest probable source of error in single crystal measurements both with polarised and unpolarised neutron beams. Extinction becomes smaller as the wavelength of the incident radiation is reduced and this is another strong reason for not using neutron wavelengths much in excess of 1 Å.

A polarised neutron diffractometer was set up at the CIRUS reactor, Trombay in 1965 using Co(Fe) as the polarising monoc' romator and incorporating a resonant flipper to flip the neutron polarisation (Satya Murthy *et al* 1969). The magnetic guide field has a

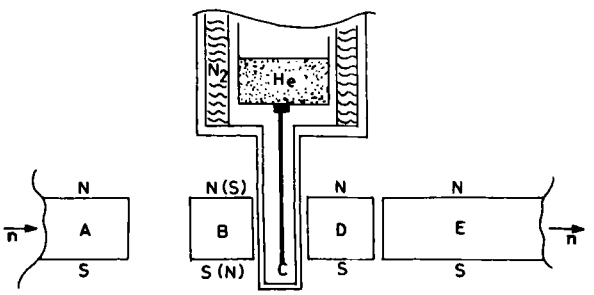

Figure 2. Non-adiabatic spin flipper system that uses an isolating sheet of superconducting niobium (see text).

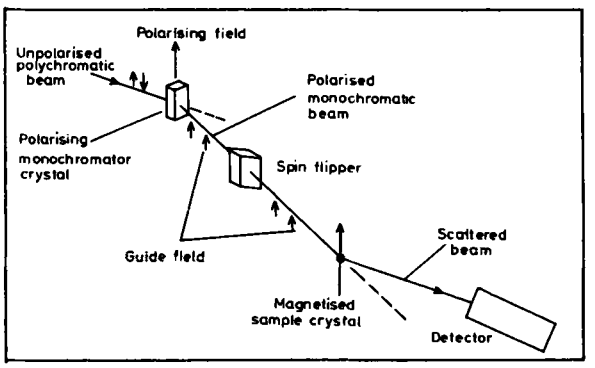

Figure 3. Schematic diagram of a polarised beam diffractometer.

Table 2. Parameters of the Trombay polarised beam diffractometer.

Neutron wavelength	0·92 A
Polarised neutron flux at sample position	2×10^4/cm^2/sec
Second order contamination	~ 1%
Polarisation efficiency	97%
Flipping efficiency	100%
Polarising field	0·3 T
Guide field	0·0121 T
Flipping frequency	355 kHz
Analysing field	0 to 2 T

provision to 'twist' the neutron polarisation vector from a direction normal to the scattering plane to the scattering plane itself. The principal parameters of the Trombay polarised beam diffractometer are listed in table 2.

6. Polarised beam in the investigation of spin density distribution and form factor studies in magnetic crystals

The most significant application of polarised thermal neutron beams has been in the detailed mapping of magnetisation density distribution and form factor studies in ferro, ferri and certain types of antiferromagnetic materials. The spatially periodic magnetic moment density at any given point (x, y, z) in the crystal can be expressed as the Fourier sum of the magnetic structure factors measured both in magnitude and sign over an ideally infinite momentum space

$$\rho(x,y,z) = \frac{1}{V} \sum_{\substack{hkl \\ -\infty}}^{+\infty} M_{hkl} \exp\left[-2\pi i \left(\frac{hx}{a} + \frac{ky}{b} + \frac{lz}{c} \right) \right]. \tag{20}$$

In practice, however, by adopting suitable averaging procedures, good accuracies can be achieved by measuring Bragg reflections up to $\sin\theta/\lambda \simeq 1\,\text{A}^{-1}$, where with polarised neutrons even small magnetic structure factors can be measured with considerable accuracy. This high sensitivity with a polarised beam is possible because in this technique one essentially measures the *interference* term between nuclear and magnetic scattering. Thus it is only with the advent of this technique that very accurate magnetic form factors and precise magnetisation density maps have emerged over the last two decades, providing us a good physical insight into the nature of magnetism in magnetically ordered materials. As a typical example, figure 4 is an illustration of magnetic moment density maps obtained by Chakravarthy *et al* (1980) in the dilute ferromagnetic alloy, $Ni_{1-x}Ru_x$.

A full discussion of the contribution made by the polarised neutron technique in the elucidation of moment density maps and form factors in magnetic materials is beyond the scope of this article. The reader is referred to a recent review by Madhav Rao (1980).

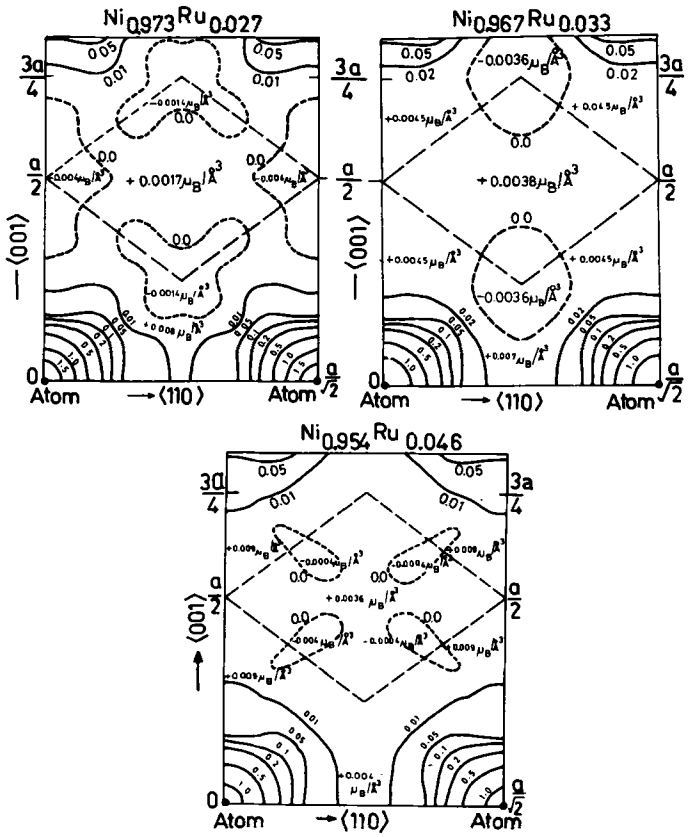

Figure 4. Section of the magnetisation density distribution in the (110) plane of $Ni_{1-x}Ru_x$ (x = 0·027, 0·033 and 0·046). One of the Wigner–Seitz cell faces shared by the atoms $\frac{1}{2}\,0\,\frac{1}{2}$ and $0\,\frac{1}{2}\,\frac{1}{2}$ is shown by the portion enclosed by the broken lines.

7. Dynamic concepts in polarisation

In §2 we discussed the method to produce polarised neutrons which has the following basic feature: it makes use of only that part of the intensity which corresponds to the projection on to the desired direction of polarisation. Neutrons having the opposite direction of polarisation are not available in the polarised beam produced, its intensity therefore being at best 50% of that of the incident beam. Recently a new method of polarising a neutron beam has been proposed (Badurek *et al* 1980) which in contrast to conventional polarisers allows in making use of 100% of the incident intensity. It exploits the fact that neutrons of different spin states differ in velocity after they have passed through an arrangement of crossed static and time-dependent magnetic fields. Provided the neutrons initially are sufficiently monochromatic, the two spin states can be separated in momentum space and be forced to point into the same spatial direction by means of a momentum-dependent spin rotation procedure (figure 5). A basic condition which has to be fulfilled is that the half width δE of the energy distribution of the incident neutron beam should be equal or less than the induced energy splitting ΔE

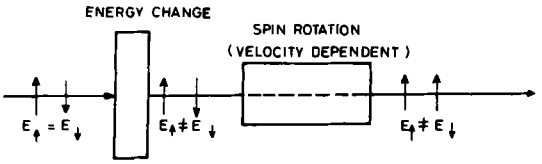

Figure 5. Principle of dynamical polarisation.

of the two spin states. A practical realization of these concepts should therefore fulfil the following essential conditions: (a) a 'device' whose interaction with the neutrons on the one hand lead to a spin-dependent energy shift of the latter but on the other hand does not remove any neutron from the beam by scattering or absorption; (b) after this 'device' a definite correlation between the spin states and the total energies of the neutrons has to be established. This implies that the energy transfer difference has to be larger than the spectral width of the incident beam. (c) finally a spin rotating device is needed which acts in an essentially energy-dependent manner on both the spin states and thus leads to a situation where all the neutrons that leave it are polarised into the same direction. The main difficulty to be overcome for an actual experimental realisation of this 'dynamic' concept is to achieve a sufficient separation in momentum space of the two different spin states. Due to the limited strengths of the magnetic fields available, the basic energy splitting process obtained by means of crossed static and time-dependent fields has to be repeated several times in order to increase the overall energy difference between the spin up and spin down components. With the present available magnet technology an energy difference of around 2μ eV seems to be feasible. Thus, to polarise a continuous beam of thermal neutrons, a very high degree of monochromaticity will have to be achieved ($\delta E/E \simeq 10^{-5}$). This technique seems to be particularly powerful, however, in the production of polarised cold and ultracold neutrons where energy spreads of 1 % or more are admissible. Badurek *et al* (1980) have shown that at pulsed sources even polychromatic neutrons can be polarised by his technique.

8. Polarisation analysis

In §5 we had discussed the use of polarised thermal neutron beams in the investigation of moment density distributions and form factors. In these studies, the polarisation of the scattered neutron beam is not measured. There is however, more physical information to be gained if the polarisation of the scattered neutrons is also analysed. In particular, the scattered beam polarisation may be changed from its initial (non-zero) value even if the target system has no preferred axis at all.

A thorough delineation of the possibilities offered by such an analysis was first made at Oak Ridge nearly fifteen years ago by Moon *et al* (1969). This polarisation analysis technique (see figure 6) employs an incident beam polarised parallel or antiparallel to a guide field whose directions in space remains constant across the sample; each incident neutron is thus in one of two possible spin eigen-states which we will denote by $1+\rangle$ and $1-\rangle$. After scattering, the beam is analysed by a flipper-polarising crystal combination, aligned parallel to the incident spin direction. Such an analyser effectively measures the Zeeman energy of the neutron by acting as a perturbation which transfers

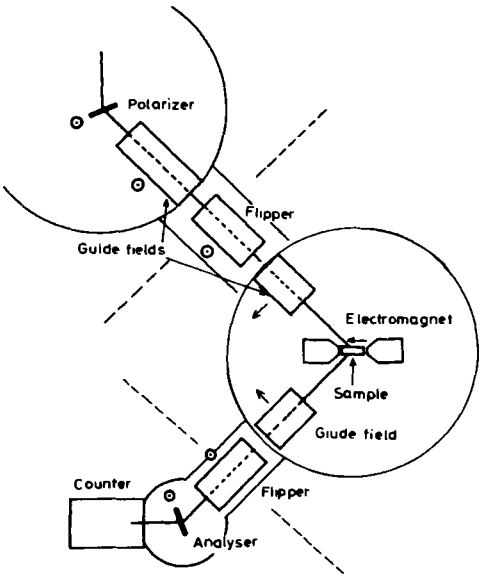

Figure 6. Schematic diagram of a polarisation analysis spectrometer.

the neutron spin to one of its eigen states. For parallel polariser and analyser directions, the available incident (i) and scattered (f) eigen states will be the same, and hence we have basically four transition probabilities: $1+\rangle_i \rightarrow 1+\rangle_f$, $1+\rangle_i \rightarrow 1-\rangle_f$ and their converses.

These transition probabilities are the four partial cross-sections, designated $(++)$, $(+-)$, $(-+)$, $(--)$, which were calculated by Moon *et al* (1969) and measured by them for a number of systems. The theory of such measurements is by no means new (see for example Schermer and Blume 1968) but the importance of an analysis in these terms is that it shows how to extract additional valuable (and often unique) information from the system under study at a minimum cost in added experimental complexity. Some of its powerful applications are in the precise determination of para-magnetic scattering and in the isothermal separation of magnetic and nuclear Bragg peaks in antiferromagnets. This technique is particularly important for a second reason: it extends the use of polarised neutrons beyond their conventional application in the study of (aligned) electronic magnetism. The neutron spin-nuclear spin interaction in spin-dependent scattering can be exploited to separate uniquely coherent from incoherent scattering or to modulate structure factors especially in hydrogenous systems. Alternatively, the neutron may have no spin interaction with the sample. We may still use its interaction with a suitably time-dependent (in the neutron's frame) external field to determine fine structure in the scattered energy spectrum as in the neutron analogue of the NMR-spin echo (§9). Yet another possibility is simply to absorb the polarised neutron to produce a polarised nucleus, which can then be used to study, for example, its own recoil defect—"in beam" NMR. For a fuller discussion on these interesting aspects one may see Hayter (1976).

9. Spin-echo spectrometry

The concept of a neutron spin-echo spectrometer was first discussed by Mezei (1972). Figure 7 shows the schematic arrangement of this spectrometer. A brief description of its principle is as follows: A linearly polarised neutron beam passes through a uniform magnetic guide field and is detected by a spin analyser aligned in the direction of the polarisation. At some point in the uniform guide field H_0 (parallel to z) a $\pi/2$ spin turn is applied after which the polarisation will precess about H_0. This neutron beam with a precessing polarisation falls on the sample S. The scattered beam now has its polarisation reversed by the π spin turner and the beam now precesses in the guide field H_0 in the *opposite* sense. A further $\pi/2$ spin turn at the end of this guide field brings the polarisation on to the analyser direction. If the field and the transit time (*i.e.* neutron wavelength) are exactly matched in the two guide fields, the full initial polarisation of the beam is recovered in the analyser. Thus, under fixed geometrical conditions, linear variations in transit time (and hence neutron wavelength) will therefore give a sinusoidal variation in the intensity transmitted by the analyser and this may be used as an extremely sensitive measure of changes in the neutron velocity. The unique aspect of this set-up is that extremely fine variations in the neutron velocity as a result of scattering from the sample is monitored *via* the change in the polarisation. If $S(Q, w)$ is the scattering law of the sample, then for a fixed momentum transfer, the measured x component of the polarisation is, to a very good approximation, given by

$$P_x = \int_{-\infty}^{+\infty} S(Q, w) \cos(wT)\, \mathrm{d}w,$$

where T, which has the dimension of time, depends linearly on the number of precessions in FP_2 and hence may be controlled by varying $|H_0|$. We thus measure the Fourier transform of $S(Q, w)$ on a time scale which overlaps with NMR, the equivalent energy resolution is of the order of 10^{-8} eV. The unique feature of the neutron spin-echo spectrometer is that such high energy resolutions are achievable even with beam monochromaticity of the order of 10 to 20% since resolutions and intensities are *fundamentally* decoupled. The neutron spin-echo offers itself as a particularly

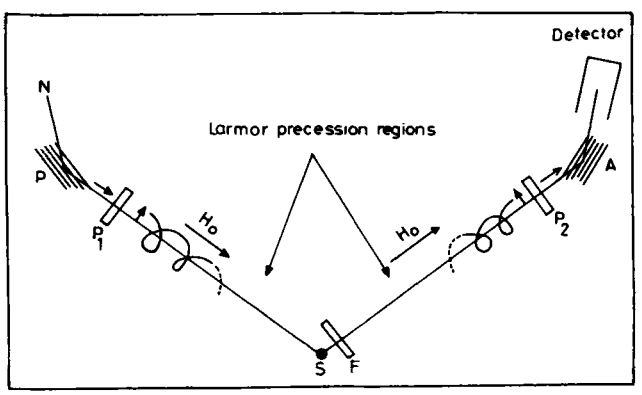

Figure 7. Schematic diagram of a focussed spin-echo spectrometer. N: Unpolarised incident beams; P, A: polariser and analyser, P_1, P_2: $\pi/2$ spin turn coils. F: π spin turn coil. S: Sample. H_0: guide field (shown solenoidal here).

interesting technique for monitoring soft modes near phase transitions, excitation near the 'freezing' temperature in spin glasses, and in the investigation of many problems in colloidal and macromolecular chemistry.

10. Conclusion

Though the main theme of this article has been the methodology of production of polarised neutrons and the 'polarisation-turning' devices, some effort has been devoted to highlight, albeit briefly, a few important physical applications of the polarised neutron beam. Some of the novel techniques discussed above are extending the usefulness of polarised neutrons to many new areas, particularly in chemistry. In other more conventional areas, new techniques of polarised neutron production should make possible many experiments which were previously limited by flux, especially in magnetic inelastic scattering.

Acknowledgements

We are grateful to Dr P K Iyengar who first pointed out to us, in the late fifties, the remarkable possibilities with polarised neutrons and set our course in their pursuit.

References

Badurek G, Westphal G P and Zeigler P 1973 *Nucl. Inst. Methods* **120** 351
Badurek G, Rauch H and Zeilinger A 1980 *Z. Phys.* **B38** 303
Bednarski S, Dobrzynski L and Steinsvoll O 1980 *Phys. Scr.* **21** 217
Blume M 1963 *Phys. Rev.* **130** 1670
Chakravarthy R, Madhav Rao L and Satya Murthy N S 1980 *Pramana* **15** 207
Delapalme A, Schweizer J, Couderchon G, Perrier de la Bathie R 1971 *Nucl. Inst. Methods* **95** 589
Fuess H, Givord D, Gregory A and Schweizer J 1979 *J. Appl. Phys.* **50** 2000
Halpern O and Johnson M H 1939 *Phys. Rev.* **55** 898
Hayter J B, Penfold J and William W G 1976 *Nature (London)* **262** 569
Hayter J B 1976 *Proc. Conf. Neutron Scattering, Gatlinburg, USA* Vol 2
Jones T J L and William W G 1977 Rutherford Laboratory Report R1 77-079A
Luschikov V I, Taran Yu V, Shapiro F L 1970 *Sov. J. Nucl. Phys.* **10** 669
Madhav Rao L 1980 in *Current trends in magnetism* (eds) N S Satya Murthy and L Madhav Rao (Bombay: Indian Physics Association)
Maleev S V 1961 *Sov. Phys. JETP* **13** 860
Mezei F 1972 *Z. Phys.* **255** 146
Mezei F 1976 *Commun. Phys.* **1** 81
Moon R M, Riste T and Koehler W C 1969 *Phys. Rev.* **181** 920
Nathans R, Shull C G, Shirane G and Andersen A 1959 *J. Phys. Chem. Solids* **10** 138
Nityananda R and Ramaseshan S 1971 *Solid State Commun.* **9** 1003
Satya Murthy N S, Somanathan C S, Begum R J, Srinivasan B S and Murthy M R L N 1969 *Indian J. Pure Appl. Phys.* **7** 546
Schermer R I and Blume M 1968 *Phys. Rev.* **166** 554
Schoenborn P, Caspar D L D and Kammerer O F 1974 *J. Appl. Crystallogr.* **7** 508
Schweizer J, Gregory A, Givord D 1979 Private Communication
Shull C G 1951 *Phys. Rev.* **81** 626
Stanford C P, Stephenson T E, Cochran L W and Bernstein S 1954 *Phys. Rev.* **94** 374
Steinsvolt O 1963 Kjeller Report KR-65
Sumaamidjaya K, Marsongkohadi, Paranjpe S K, Murthy M R L N and Satya Murthy N S 1983 to be published.
Van Laar B, Maniawski F and Mijnarends P E 1976 *Nucl. Inst. Methods* **133** 241
Williams W G 1974 Rutherford Lab. Report RL-74-036